ELSEVIER

Journal of Nuclear Materials 283–287 (2000) 60–69

journal of nuclear materials

www.elsevier.nl/locate/jnucmat

Impact of irradiation effects on design solutions for ITER diagnostics

S. Yamamoto *, T. Shikama [1], V. Belyakov [2], E. Farnum [3], E. Hodgson [4], T. Nishitani [1], D. Orlinski [2], S. Zinkle [3], S. Kasai [1], P. Stott [4], K. Young [3], V. Zaveriaev [2], A. Costley, L. deKock, C. Walker, G. Janeschitz

ITER Joint Central Team, Boltzmannstraße 2, 85748 Garching, Germany

Abstract

An overview of the results of the irradiation tests on diagnostic components under the ITER technology R&D tasks and the solutions for the present diagnostic design are given in the light of these results. A comprehensive irradiation database of diagnostic components has been accumulated and permits conclusions to be drawn on the application of these components in ITER. Under the ITER technology R&D tasks, not only has work been shared among four home teams, but also several bilateral collaborations and round-robin experiments have been performed to enhance the R&D activities.

1. Introduction

In order to evaluate and establish an ITER-relevant database to support the design of the diagnostic systems [1] and their implementation [2,3], irradiation tests on ceramics, wires/cables, windows, optical fibres and mirrors/reflectors have been performed under the ITER technology R&D tasks. These are key components of diagnostic systems and are expected to be used in relatively high-irradiation environments [4–7]. A comprehensive irradiation database has been accumulated and permits conclusions to be drawn on the application of these components in ITER [8,9].

Many technical meetings and workshops were held to examine the irradiation test plans and evaluate irradiation test results of each home team. These meetings or workshops provided the opportunity for radiation experts, diagnostic engineers and diagnosticians to develop a common base for understanding radiation effects on diagnostic components.

In general, irradiation tests start with a general survey of suitable materials. As the design of the diagnostic systems progresses, the irradiation tests will focus on the solution of well-identified problems and irradiation of prototype assemblies including sensors (magnetic coils, bolometers, pressure gauges, etc.) and transmission components (window and mirrors/reflectors assemblies, optical feedthroughs, vacuum electric feedthroughs, remote handled electrical connectors, etc.).

Under the ITER technology R&D tasks, not only has the work been shared among four home teams, but also several bilateral collaborations and round-robin experiments have been performed to enhance the R&D activities.

Radiation aspects of design solutions for selected diagnostic systems are examined based on the ITER maintenance scheme, the irradiation database for physical and mechanical properties and the required signal-to-noise ratio (SNR) of the system taking into account the ITER irradiation environment and irradiation shielding capability for diagnostic components.

An overview of the results of the irradiation tests on diagnostic components and the solutions for the present diagnostic design are given in the light of these results.

* Corresponding author. Tel.: +49-89 3299 4427; fax: +49-89 3299 4165.

E-mail address: yamamos@itereu.de (S. Yamamoto).

[1] JA Party, ITER Home Team.

[2] RF Party, ITER Home Team.

[3] US Party, ITER Home Team.

[4] EU Party, ITER Home Team.

0022-3115/00/$ - see front matter
PII: S0022-3115(00)00157-4

2. Physical and mechanical properties of key components

Each location of the component and the radiation shield configuration for the component must be designed taking into account the lifetime and required SNR of the diagnostic system. We require that the design of the diagnostic systems maximises the lifetime of the diagnostic components installed in the cryostat. The minimum requirement is that components, for example, in the diagnostic divertor cassettes and in the diagnostic plugs, survive longer than the lifetime of these in-vessel components, so that the diagnostic component will not be the driver for replacing the related in-vessel component [8]. Design solutions for selected diagnostic systems have been obtained by an iteration process between radiation effects, the desired performance of the diagnostic and the environment.

The fast neutron flux (>0.1 MeV) and ionisation dose rate at the first wall of ITER are 3×10^{18} n/m^2/s and 3×10^3 Gy/s during operation with a wall load of 1 MW/m^2, respectively. A total fluence of 10^{25} n/m^2 leads to about 1 dpa (displacement per atom) damage in ceramics. Therefore, a total damage of 3 dpa and a total ionisation dose of 3×10^{10} Gy in ceramics are expected at the first wall at the end of the ITER life for a total fluence of 0.3 MWa/m^2. Intensities of expected radiation dose rates on diagnostic components depend on positions and specific surrounding geometries, but about 10^{16-18} n/m^2/s fast neutron flux and 1–10^4 Gy/s ionising radiation dose rates should be expected in the temperature range of 300–700 K.

Primary candidate materials and irradiated materials are shown in Table 1 [8].

2.1. Ceramics and wires/cables

The quality of electrical insulation in ceramics is one of the key issues for ITER diagnostic systems. Insulating ceramics will be used in feedthroughs, connectors, mechanical supports and general stand-offs, mineral-insulated (MI) cables and their seals, substrates of bolometers [10,11], and other sensor devices such as pressure gauges [12]. Ceramics windows are also used in diagnostic systems and heating/current drive systems [13].

For ceramics, radiation-induced conductivity (RIC), radiation-induced electrical degradation (RIED, which is a permanent degradation observed in ceramic insulators under applied voltage), dielectric, thermal and mechanical properties, and tritium diffusion have been studied. For wires/cables, RIC, RIED, radiation-induced electromotive force (RIEMF) between sheath and centre conductor of MI cables and conductor resistance have been measured.

For cables/wires, RIC, RIED, RIEMF and dielectric breakdown strength have been measured. Equilibrium coils made of mineral MI cables require an insulating conductivity of less than 10^{-6} S/m (preferably much less i.e., 10^{-7} S/m) leading to an acceptable parallel loading of the integrator input. Effects of RIEMF in magnetic probes which are part of the long-time integrator circuit are important [14]. Sometimes, degradation of insulation resistance along the surface of cable termination due to gas conduction or surface contamination under irradiation is observed. Reliable cable termination techniques with low leakage currents for MI cables should be developed (Fig. 1).

2.2. Windows

The wavelength regions to be used for plasma diagnostics are:

1. 200–350 nm (ultra-violet measurements);
2. 350–700 nm (visible spectral measurements);
3. 700–1200 nm (near infra-red measurements);
4. 3000–11 000 nm (infra-red measurements);
5. 0.1–10 mm/3000–30 GHz (ECE, microwave measurements);
6. 5–100 keV (soft X-ray diagnostics).

Window assemblies must be vacuum tight to UHV standards and also be able to withstand the 0.2 MPa pressure rise of a LOCA. Windows transmit optical and microwave signals through the tritium confinement barriers. Optical windows will be diffusion bonded to metal ferrules. Tests and experience have shown this to be stronger than the window material and able to withstand 0.5 MPa in either direction [3].

Key testing issues of diagnostic windows are illustrated in Fig. 2 [8]. Some issues for windows are common with ceramic issues. For potential window materials, the optical properties including radioluminescence and optical transmission have been studied. In addition to enhanced tritium diffusion, there is a possibility of enhanced tritium leaks due to microcracking in the ceramics-to-metal joints due to sub-critical crack growth (SCCG). For applications to LIDAR Thomson scattering systems [15], synergetic effects of high-power laser-beams and irradiation and/or surface degradation are very important from mechanical damage point of view.

2.3. Fibre optics

For a large variety of optical diagnostics, it is extremely desirable to be able to use fibre optic transmission close to the plasma region to take advantage of the limited spatial access, easy alignment of optical components under relative movements between each component, and a vacuum boundary that can be shown to pose a smaller safety problem in the event of failure. In order to introduce optical fibres through the vacuum vessel ports, metal-jacketed fibres were developed, which

Table 1
List of candidate materials and irradiated materials

Diagnostic components	Primary candidate materials	Irradiated materials
Ceramics for insulator	• Alumina (Al_2O_3) • High purity silica glass	Alumina, silica glass, BeO, AlN, Si_3N_4, $MgAl_2O_4$, MgO, pyrolitic BN
Window-1 (300–1200 nm)	• High purity quartz and fused silica (SiO_2) • Single-crystal alumina (sapphire)	Sapphire, quartz, fused silica glass KU quartz[a]
Window-2 (2000–5000 nm)	• High purity quartz and fused silica (SiO_2), same as shorter wavelength	Single-crystal alumina (sapphire), fused silica
Window-3 (10 μm)	• ZnSe	
Window-4 (100 μm–10 mm)		Diamond, silica
Fibre optics UV to IR (300 nm–5 μm)	• Low OH, pure silica core, F-doped cladding, aluminium jacket • Fluorine-doped core fibre • Hydrogen-treated fibres • Gamma-hardened fibre	Quartz, core (pure silica)/clad (F-doped silica) • Improved type, core (pure SiO_2)/clad (F-doped SiO_2), low OH-content (from 1 to 100 ppm) two samples, Al jacket or high OH-content (300 ppm) polymer or Al jacket • F-doped SiO_2 core • Gamma-hardened fibres • Single-crystal fibres
Mirrors/reflectors-1 front-end mirror (visible/infra-red)	• Copper (Cu) • Stainless steel (St.St.) • Beryllium (Be) • Pure aluminium (Al) • Molybdenum (Mo)	Mo, Cu, St.St., Be, Al, Ti, W, graphite
Mirrors/reflectors-2 secondary mirror (UV/visible/infra-red)	Aluminium-coated spinel ($MgAl_2O_4$)	
Mirrors/reflectors-3 high-power laser mirror (laser mirror and collection systems) (UV/visible/infra-red)	Dielectric mirror (multilayer mirror) • HfO_2/fused silica • TiO_2/fused silica	High-power laser mirror (laser mirror and collection systems) HfO_2/SiO_2, ZrO_2/SiO_2, TiO_2/SiO_2
Mirrors/reflectors-4 (X-rays 1–500 Å)	• Various diffraction crystals • Multilayer mirror/LSM	• Crystals (LiF, mica, Ge, Si, SiO_2, pyrolytic graphite, pentaeritric potassium biphtalate, rubidium biphtalate) • Multilayer mirror (Cr/C, W/Si, Fe/Cr, $MoSi_2$/Si, Mo/Si), LSMs (Mo/Si, W/B_4C and W/C)
MI cables	• MgO, stainless steel sheath, nickel or copper centre with diameter from 0.3 to 2.3 mm OD • Other insulator	• Al_2O_3, MgO, MgO-insulation; Ni, NiCr, SS-wire; SS-shield • Ten different improved MI cables
Ceramic coated wire		• $70MgAl_2O_4 + 30Al_2O_3$, plasma spraying insulation, Ni-wire

[a] Round Robin material.

are high-vacuum compatible and bakeable to 350°C. Irradiation effects on solder between the optical fibre and the metal flange remain to be investigated [16].

Important issues for ITER diagnostics are radiation resistance of optical fibres especially for the visible region, and their application in the vicinity of the first wall. Irradiation effects on radioluminescence and degradation of optical transmission due to permanent and transient absorption have been characterised.

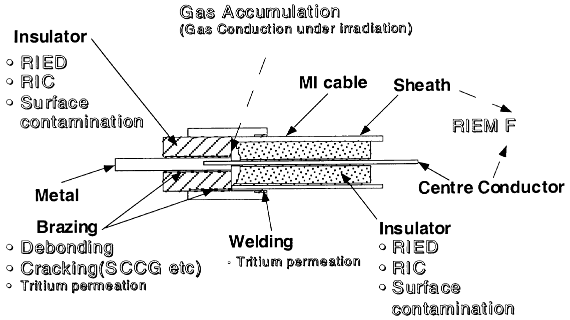

Fig. 1. Example of MI cable terminations and key issues.

There are many methods or effects for improving characteristics of optical fibres under irradiation. Pre-gamma irradiation techniques, photo bleaching, thermal bleaching, hydrogen treatment (hydrogen loading) and doping have all been investigated under gamma and neutron irradiation. The effect of temperature on radioluminescence and optical transmission under irradiation, and thermal annealing effects, have also been investigated. Key parameters of optical fibres, which affect radiation resistance, are as follows: fibre composition (dopants, OH-content, impurities, cladding type), fibre fabrication (manufactured drawing speed and temperature) and preform fabrication. Before irradiation tests, these characteristics should be specified.

Optical fibres will be employed in such a way that only a few meters will be exposed in a high-radiation flux region, thus the radiation-induced optical absorption will be confined to this region and may be described in decibel per metre. Permissible loss will be in the range of $<10^2$ dB/m.

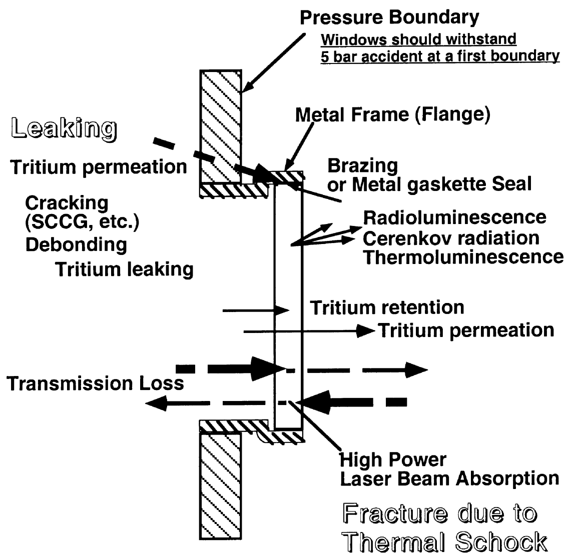

Fig. 2. Key issues of window assemblies.

2.4. Mirrors/reflectors

Since lenses and windows may not be employed close to the plasma because of the severe degradation, the first optical element will be a 'first mirror'. These first mirrors will experience the most severe environmental conditions in the ITER device. The first mirror is potentially in the first wall radiation environment. Irradiation tests have been performed on metal bulk mirrors, single-coated mirrors, dielectric coatings on ceramics for high-power laser beams, layered synthetic microstructures (LSMs) [17] for UV reflectors, crystalline materials for X-ray spectroscopy, and graphite elements for sub-millimeter plasma diagnostics.

3. Summary of principal irradiation test results and impact on ITER diagnostic design solution

In this section, principal irradiation test results on key components are described. Based on the irradiation test results, recommended materials and maximum allowable dose or dose rates for these materials were identified. These results are summarised in Table 2. In order to clarify the impact of irradiation effects on ITER diagnostic design solutions, magnetic systems and LIDAR Thomson scattering systems are examined based on these irradiation test results and the issues which should be resolved in the future are identified.

3.1. Ceramics and wires/cables

3.1.1. Test results

In the course of extensive studies of RIED, international round-robin tests proposed for reliable measurements of electrical conductivity under irradiation [18–20]. Extensive experiments have been carried out successfully, using a standardised measuring technique that was established by a group of active researchers [21].

Bulk RIED can be produced in Al_2O_3 during electron irradiation [22,23]. However, definite evidence of catastrophic RIED has not been observed in Al_2O_3 during numerous ion or fission neutron irradiations (up to 3 dpa) [24] to damage levels much higher than those achieved in electron irradiation studies. However, further analysis has revealed moderate to substantial electrical degradation in some of the sapphire samples [25]. Clearly material type is an important parameter, and the high purity material (sapphire) appears to be more susceptible to degradation. It should be noted here that reactor experiments were carried out in helium atmosphere, while charge particles irradiations were performed in vacuum.

Reliable extensive data on RIC have also been accumulated. The measured RIC under 14 MeV neutron irradiation using the fusion neutron source (FNS) was

Table 2
Recommended materials and maximum allowable dose or dose rates

Diagnostic components	Recommended materials	Accumulated effects	Dynamic effects
Ceramics (electrical insulators)	Single-crystal sapphire and polycrystal alumina (Al_2O_3)	3 dpa in helium atmosphere (RIED: no catastrophic degradation)	10^4 Gy/s (RIC: <10^{-6} S/m)
Wires/cables	MI-cables: SUS, Inconel (sheath)/MgO, Al_2O_3 (insulator)/Cu, Ni (centre conductor)	1.8 dpa (RIED: no catastrophic degradation)	10^4 Gy/s (RIC: <10^{-6} S/m) 10^3 Gy/s (RIEMF: <10 V)
Windows	Fused silica/quartz (400–1200 nm)	10^{-3} dpa (transmission; 5% degradation: 8 mm^t)	Radioluminescence: 10^7 photons/Gy Å sr cm^3 at 410 nm
	Sapphire (800–5000 nm)	0.4 dpa (transmission; no degradation: 1 mm^t)	Radioluminescence: 10^{10} photons/Gy Å sr cm^3 at 410 nm
Optical fibres	Pure silica (core)/F-doped (clad)/Al jacket (visible region)	10^7 Gy (transmission: 2–2.5 dB/m) 10^{-2} dpa (transmission: 10 dB/m)	Radioluminescence
	Pure silica (core)/F-doped (clad)/Al jacket (IR region)	1 dpa (transmission: 10 dB/m)	Radioluminescence
Mirrors/reflectors	First mirrors: metal (Cu, W, Mo, St.St., Al)	40 dpa (Cu) (reflectivity: no degradation)	
	First mirrors for LIDAR: single-coated (Rh/V)?		
	Dielectric mirrors: (HfO_2/SiO_2, TiO_2/SiO_2)?	<10^{-2} dpa (flaking, blistering)	
	LSMs: (Mo/Si, W/B_4C and W/C)?	<10^{-2} dpa (the shift of the peak reflectivity to shorter wavelength)	
	X-ray crystals: (Ge, Si, SiO_2, Graphite)	10^{-2} dpa	

proportional to the electronic excitation dose rate, and fell within the scatter band of the RIC-dose rate relation obtained from X-ray, γ-ray, electron, ion and fission neutron irradiation [26].

A completely new demonstration of dynamic irradiation effects has been presented for the mechanical properties of alumina. SCCG was measured under constant load with and without exposure to radiation at 1.5 Gy/s. The time to failure for a given ratio of applied stress to critical stress was found to increase in some cases, and to decrease in other cases, compared to unirradiated samples [27].

3.1.2. Impact on design solution

The present data indicates that the long-term volume degradation of electrical insulating ability should not impose serious technological problems at least in the short and middle term development of fusion devices such as ITER. Additional problems which have been identified such as surface conductivity [28], insulator cracking [29] and electric charging effects [30] require further investigation to determine the physical mechanisms responsible for associated RIED-like electrical degradation, and to assess their possible influence on the insulator performance and lifetime.

No catastrophic RIED was observed up to 1.8 dpa in MI cables. The important factors of RIC are the operating temperature, irradiation dose rate, and material type. The RIC was quantified and should not be a problem for magnetic measurements. However, RIC effects on thin ceramic films of a bolometer are still an open issue.

Dimensional stability of magnetic coils made of MI cables (MI-coil) have been investigated by measuring inductance change of the magnetic coils. No inductance change of a magnetic coil made of MI cables was observed up to a neutron fluence of 0.1 dpa (10^{24} n/m^2; $E > 0.1$ MeV) [31]. One of the key issues is the effect of asymmetry of the RIEMF on the long pulse integrator. Two sets of these two coil coaxial systems with four different diameter of centre leads and insulators but with the same diameter of outer sheath were irradiated in the

JMTR fission reactor under JA/US collaboration. The MI-cables with the fattest centre lead showed the lowest RIEMF as well as the highest electrical conductance along the centre lead [32].

3.2. Window

3.2.1. Irradiation test results

No irradiation effects on optical absorption of sapphire windows with 10 mm thickness for IR regions from 850 to 5000 nm was observed up to a fast ($E > 0.1$ MeV) neutron fluence of 5×10^{23} n/m^2 (0.05 dpa) at 470 K, whereas transmission is reduced to 10% at 400 nm and 60% at 600 nm [33].

No significant irradiation effects on optical absorption of fused silica glass KU-1 with 8 mm thickness for visible regions (from 350 to 850 nm) were observed up to 10^{22} n/m^2. Transparency in the wavelengths from 450 to 650 nm decreased by 5% to 15% in the range of the fluence from 10^{22} to 5×10^{23} n/m^2 [34,35].

Radioluminescence, on the other hand, associated with ionising radiation is very strong in sapphire (compared with silica) and will be a problem for radiation levels above 100 Gy/s. Quantitatively evaluated radioluminescence data is now available. Radioluminescence from the two candidate materials of sapphire and KU-1 fused silica for an optical window was measured under 2 MeV electron radiation [36]. Large radioluminescence is observed in sapphire, mainly generated by oxygen vacancies, so-called F and F^+ centres. Also, radioluminescence peaks caused by a small amount of impurities such as gallium and chromium are clearly observed. Displacement damage increases the intensity of radioluminescence caused by oxygen vacancies. Unirradiated fused silica showed very weak radioluminescence, and Cerenkov radiation dominates, though for some grades there are several radioluminescence peaks in the wavelength range of 300–800 nm, with the radioluminescence peak at about 450 nm increasing its intensity substantially as radiation dose increases. However, KU-1 material shows very few peaks.

Efficiency of induction of radioluminescence depends on radiation fields including electron beams, 14 MeV neutrons and gamma-rays. When they are compared at an equivalent ionising dose rate of 1 Gy/s, gamma-ray radiation is most effective at inducing F-centre radioluminescence [8].

3.2.2. Impact on design solution

Fused silica glass or quartz windows should be used in spectroscopic systems for visible regions, and sapphire windows should be used for IR regions.

From the viewpoint of radioluminescence, fused silica has an advantage over sapphire as a window material. On the one hand, optical absorption in sapphire is insensitive to gamma radiation and only displacement damage associated with neutron irradiation induces notable absorption. On the other hand, optical absorption in silicas (covalent-bonding) is sensitive to gammas (ionising irradiation) as well as to atomic displacements. Thus, under high-flux ionising-radiation, sapphire will have some advantages over fused silica. A crystal quartz is more resistant to radiolysis than a fused silica.

Availability in quantity and in sizes of window materials made of fused silica (synthesised silica especially for large windows and optical fibres) should be considered.

Radiation associated degradation does not appear to be a problem for the metal to ceramic seals, assuming that the window assembly will reach less than 10^{-2} dpa. Existing irradiation data for jointing/bonding (alumina, macor, spinel, alon, sialon) shows good radiation resistance up to 4×10^{-2} dpa (3.8×10^{23} n/m^2) [37]. Volume changes in SiO_2 materials, especially fused silica, must be taken into account even at low neutron fluence at elevated temperatures.

Sealing to zinc selenide still remains to be demonstrated within the current window development programme. Using a new bond technique for a window seal with a spring seal on the glass edge, a window assembly was fabricated [38]. The window assembly will be tested under gamma irradiation in order to clarify the effect of SCCG on the glass.

In the case of diamond, excellent material grades have been developed in the ECRH programme (at 145 GHz), which may possibly be used for diagnostic windows from the GHz region right up to the IR/visible range [39].

Unexpected technical problems for the whole system, such as tritium diffusion and retention at the ceramic to metal seal, have to be assessed. Irradiation tests of complete window assemblies may be needed to quantify the overall lifetime, where safety aspects must be fully considered in the tests.

The LIDAR Thomson scattering system is one of the optical diagnostics requiring a large access hole to allow a high-enough photon collection efficiency. The shielding block with the labyrinth in which several mirrors are installed reduces the neutron streaming to the vacuum vessel port structure and to the main Tokamak coils to a level close to that of the unbroken shield and allows fused silica glass KU-1 windows to be used at the vacuum boundary.

Based on the database on transparency of fused silica glass KU-1 for the LIDAR, the following conclusions can be drawn:

1. radioluminescence from fused silica glass KU-1 has no effect on SNR in the concerned wavelength range, and
2. the window transparency will keep the required value during the ITER lifetime.

Radiation-induced background absorption, causing a loss in transmission of only a few percent of about 10^{-3}, could be a problem leading to mechanical breakdown. This is now being examined by the EU and RF Home Teams.

3.3. Fibre optics

3.3.1. Irradiation test results

Plasma diagnostics in TFTR tokamak revealed drastic dynamic irradiation effects in optical fibres [40]. Operating of silica core fibres at >350°C (or periodic heating) appears to be a promising way to substantially reduce the absorption for a relatively low neutron fluence. The effect of temperature on radioluminescence was also studied, and was very small in the case of fused silica. This result is consistent with the bulk of radioluminescence being composed of Cerenkov radiation and a temperature-independent peak at 450 nm [41].

Hydrogen treatments (hydrogen loading) applied to KS-4V fibres with extremely low OH (0.5 ppm) and low Cl (<20 ppm) contents in their cores showed remarkable improvement of radiation resistance under gamma radiation. The KS-4V fibre showed a rather flat induced loss spectrum in the visible region at a level of 2–2.5 dB/m for gamma-doses of about 10^7 Gy [42,43]. KS-4V has been chosen as a round-robin material, and should be fully tested for radiation-induced absorption and emission, particularly under neutron associated irradiation.

Neutron-induced absorption in aluminium-jacketed fibres was measured. Pure silica core fibres with low OH content have an induced loss in the wavelength region >400 nm less than 10 dB/m up to a neutron fluence of 1.6×10^{20} n/m^2 and in the wavelength region >800 nm less than 10 dB/m up to a neutron fluence of 10^{25} n/m^2 (1 dpa) with ionising dose of about 10^{10} Gy. Effectiveness of fluorine (F) doping and successive heat treatment were shown, which will also cure defects in heavily deformed fused silica. The fibre showed radiation-induced loss of about 20 dB/m in the visible region at a total fast neutron fluence of about 10^{24} n/m^2 [44].

3.3.2. Impact on design solutions

Accumulated results indicated that the radiation-induced loss could be less than a few tens dB/m in the wavelength region of 800–1200 nm for some developed optical fibres [8] with a fast neutron fluence of 10^{25} n/m^2 and ionising radiation dose of 10^{10} Gy.

Behaviours of optical fibres are excellent in the IR region (low absorption and low radioluminescence). Serious technical problems are not anticipated and suitable fibres already exist. The main problem will be in the associated electronics in an optical communication system.

Radiation-induced optical absorption will be a general problem at wavelengths shorter than 500 nm. A sapphire-core optical fibre may be better for ITER application, especially at places, where gamma radiation effects are dominant. Sapphire is well-known to be immune to pure electronic excitation irradiation, whereas, fused silica is known to be susceptible to radiolysis. However, radioluminescence will increase especially in the blue/UV region due to improved transmission (lower absorption).

Isochronal annealing results suggests that operating temperatures as high as 600°C may not reduce neutron damage in pure-silica core or weakly-fluorine-doped silica fibres. Similar results were obtained for the windows under gamma radiation. Temperature effects are not clearly understood yet. Annealing effects and benefits of elevated-temperature-operation (>500 K) need discussion by specialists.

More detailed, specific and extensive studies, including manufacturing processes, are needed before final conclusion can be made for application of optical fibres in ITER.

Based on today's knowledge, it is recommended to use optical fibres as follows: during operation optical fibres for the IR regions can be used inside the cryostat but optical fibres for visible regions can only be used outside the bioshield [8]. However, this recommendation seems to be very conservative. Taking into account the above-mentioned recent experimental results, there is a possibility to use the optical fibres for the visible region inside the cryostat during operation, which requires further investigation.

3.4. Mirrors/reflectors

3.4.1. Irradiation test results

Reflectivity at relevant wavelengths of various types of mirrors/reflectors was measured [8]. For single-coated mirrors and dielectric mirrors, adhesion of coated materials on mirror substrate was examined. For X-ray crystals, interplane distance and width and form of diffraction lines were measured.

Copper specimens were irradiated by Cu^+ ions of 1 or 3 MeV energy up to 50 dpa. No degradation in reflectivity was observed up to 40 dpa [45]. Molybdenum corner cube reflectors (CCR) were irradiated up to 1.4×10^{24} n/m^2 [33] and no adverse effects were also observed.

Post-irradiation measurements of LSMs for soft X-ray reflectors were completed. They were irradiated up to 1.1×10^{23} n/m^2 (0.01 dpa). A shift of peak reflectivity to shorter wavelength regions and reduction of 20% in the reflectivity of the shifted peak were observed.

Reflectivity measurements were completed on dielectric-coated mirrors irradiated up to 1.1×10^{23} n/m^2 with temperature cycled between 60°C and 270°C in LASREF [46]. Of the five types of mirrors irradiated, three showed flaking or blistering of the coating and two showed little mechanical damage.

Some organic X-ray crystals change their characteristics at a relatively low fluence level. However, inorganic crystals including Ge, Si, SiO_2 and graphite do not have a change in their reflectivity, interplane distance and width and form of diffraction lines up to 10^{23} n/m^2. Mica monocrystals preserve their characteristics up to 10^{22} n/m^2 [47].

3.4.2. Impact on design solution

Metal mirrors are preferable for first mirrors in the ITER radiation environment. There is a possibility that it will not be necessary to change the mirrors close to the first wall during the ITER lifetime if other adverse effects of sputtering, evaporation or coating are not too serious.

In fact, reflection coefficients of copper mirrors are very sensitive to sputtering [48]. For the wide-angle plasma viewing system [3] and divertor viewing system [49], the front-end mirrors need to be very close to the plasma. Effects of surface morphology due to sputtering and deposition are under study.

The design of mirror assemblies to reduce mirror distortion is very important. Displacement damage will cause configuration distortion through swelling and differential growth. Non-uniform nuclear heating will also cause configuration distortion. A JMTR radiation-test of a molybdenum corner cube mirror showed large dynamic increase of reflection loss during reactor operation [33]. This can be interpreted to mean that a configuration distortion caused by nuclear heating degraded optical behaviour of the mirror. Several heat removal techniques for mirror assemblies are under consideration [3].

Displacement damage will cause configuration distortion through swelling and differential growth. Dielectric mirrors and LSMs should be used in well-shielded locations and under temperature control.

4. International collaboration

International collaboration through the ITER EDA and related activity through the International energy agency (IEA) has played a crucial role in mobilising and focusing ceramics studies to establish an extensive reliable database for designing diagnostic components. Round-robin experiments on Wesgo 995 polycrystalline alumina (the IEA reference ceramic material), fused silica glass KU-1 (distributed by Russia) and Anhydroguide (low OH) fibre (distributed by USA) were performed by the four ITER Home Teams using various kinds of irradiation sources [8]. Further round-robin experiments on fibres will be performed. The candidate materials are KU-1 and KS-4V fibres from Russia and fluorine (F)-doped fibres from Japan.

Studies of irradiation effects in prototypical components are resource-consuming enterprises, and they tend to produce complicated results that cannot be easily analysed into elementary and fundamental processes. For the effective analysis, well-designed irradiation tests are essential. International collaborations under ITER R&D tasks also play an indispensable role there. The EU/JA collaboration on irradiation tests on bolometers and the JA/US collaboration on irradiation tests on magnetics have started. Laser-beam transmission tests under electron irradiation will be carried out for optical windows in EU under EU/RF collaboration. There, synergetic effects of laser-beam bombardments and electron irradiation will be examined in mechanically constrained conditions.

5. Summary and discussions

Eight years of effort in ITER diagnostics-related tasks has seen the international collaborations advance from the initial formal and rather cold situation to the present warm and maturing open state. The process of improvement in effective international collaboration is clearly showing the importance of personal contact in establishing confidence and trust between the people. The ITER diagnostic-related task meetings have made a fundamental contribution to cultivating warm human relationships among participating groups, which has and will be essential for successful international collaboration.

The following irradiation issues have still to be resolved for ITER diagnostic systems in the near future.

5.1. Ceramics

Roles of electronic excitation and atomic displacement should be examined further. One proposed mechanism for RIED is an electric-field induced radiolysis. The process of radiolysis claimed to be a possible cause of the permanent electrical degradation in ceramic insulators is not clearly understood yet.

Behaviour of electrical conductivity in ceramics should be examined in detail to understand fundamental processes of electrical conductivity under high-dose rate irradiation. Charge redistribution and resultant spatial charge-up and electromotive force between different materials, non-ohmic behaviour (which may be caused by interfaces between different materials), etc. should be examined.

5.2. Wire/cables and magnetic coils

Irradiation effects on remote handled electrical connectors and reliable cable termination techniques with low leakage currents for MI cables should be investigated.

Origin of the RIEMF has not been understood yet. Measurements of the radiation-induced noise including the RIEMF and any radiation-induced drifts in the long pulse integrator are underway under JA/US collaboration.

5.3. Seals and feedthrough

Windows, electric feedthroughs and optical feedthroughs constitute very important vacuum and tritium barriers in diagnostic systems. A window seal design is required to accommodate the high-bakeout temperature of 250°C. Windows as a first vacuum barrier must withstand a 2 bar accident.

Windows for applications in the ultra-violet wavelength region and for laser-beam transmission have still problems related to substantial radiation-induced optical loss. Laser-beam transmission tests under electron irradiation will be carried out for optical windows in the EU under EU/RF collaboration. There, synergetic effects of laser-beam bombardments and electron irradiation will be examined in mechanically constrained conditions.

5.4. Mirrors/reflectors

Irradiation damage threshold of dielectric mirrors and LSMs should be investigated.

Laser damage threshold in irradiated dielectric mirrors or single-coated mirrors will be performed.

Several heat removal techniques for mirror assemblies are under consideration. Validity of proposed techniques will be examined under irradiation environments.

A serious concern is that a reflection coefficient will be degraded by sputtering by low energy neutrals. Effects of surface morphology due to sputtering and deposition are under study in RF and JA Home Teams.

5.5. Bolometers

The JET-type bolometer made of mica substrates, usable at elevated temperatures of 300°C, will be tested under neutron irradiation under JA/EU collaboration. A few candidates of substrate materials, Si_3N_4, AlN, Al_2O_3 or $MgAl_2O_4$ for the JET-type bolometer were proposed for further irradiation tests.

5.6. Pressure gauges

ITER-relevant pressure gauges will be developed based on the ASDEX-type pressure gauge. Irradiation effects on the mechanical strength of hot cathodes should be addressed. Parasitic signals due to RIC, surface leakage current due to surface contamination, degradation or gas ionisation due to tritium or gamma irradiation will be evaluated.

Acknowledgements

This paper was prepared as an account of work performed under the agreement among the European atomic energy community, the Government of Japan, the Government of the Russian Federation, and the Government of the United States of America on co-operation in the engineering design activities for the International thermonuclear experimental reactors (ITER EDA agreement) under the auspices of the International atomic energy agency (IAEA).

References

[1] A. Costley, K. Ebisawa et al., Overview of the ITER diagnostic system, in: Diagnostics for Experimental Thermonuclear Fusion Reactors, vol. 2, Plenum, New York, 1998, p. 41.

[2] G. Janeschitz, C. Walker et al., Integration of diagnostics into the ITER machine, in: Proceedings of the 17th IAEA Fusion Conference, Yokohama, 1998.

[3] C. Walker, S. Yamamoto et al., Nuclear aspect of diagnostics, in: Proceedings of the Fifth International Symposium on Fusion Nuclear Technology, 19–24 September, 1999, Rome, Italy, to be published.

[4] T. Shikama, K. Yasuda, S. Yamamoto, C. Kinoshita, S.J. Zinkle, E.R. Hodgson, J. Nucl. Mater. 271&272 (1999) 560.

[5] T. Shikama, S.J. Zinkle et al., Dynamic irradiation effects in electrical conductivity of ceramic insulators, in: Proceedings of the 17th IAEA Fusion Conference, Yokohama, 1998.

[6] E.R. Hodgson, Radiation problems and testing of ITER diagnostic components, in: Diagnostics for Experimental Thermonuclear Fusion Reactors, vol. 2, Plenum, New York, 1998, p. 261.

[7] S. Yamamoto, L. deKock et al., Irradiation tests on ITER diagnostic components, in: Diagnostics for Experimental Thermonuclear Fusion Reactors, vol. 2, Plenum, New York, 1998, p. 269.

[8] S. Yamamoto, ITER Design Description Document 5.5M: Radiation Effects.

[9] Irradiation tests on diagnostic components, Reports of four Home Teams for ITER Technology R&D Tasks of T28 (reported in 1995) and T246 (reported in 1998), to be published.

[10] R. Reichle, M. Di Mao, L.C. Ingesson, K.F. Mast, Progress of the reference design for ITER bolometers and development of a high performance alternative, in: Diagnostics for Experimental Thermonuclear Fusion, vol. 2, Plenum, New York, 1998, p. 389.

[11] T. Nishitani, E. Ishitsuka, T. Kakuta, H. Sagawa, K. Noda, Y. Oyama, T. Iida, T. Sugie, H. Kawamura, S. Kasai, Fus. Eng. Des. 42 (1998) 338.

[12] G. Haas, H.-S. Bosch, D. Coster, L. deKock, J. Neuhauser, R. Schneider, J. Schweinzer, Pressure gauges and neutral pressure measurement in ITER, in: Diagnostics for Experimental Thermonuclear Fusion Reactors, vol. 2, Plenum, New York, 1998, p. 559.

[13] R. Heidinger, A. Ibara, J. Mollá, J. Nucl. Mater. 258–263 (2000) 1822.
[14] S. Bender, private communication and in Ref. [8].
[15] P. Nielsen, L. deKock, C. Gowerrs, F. Oritto, H. Saltzmann, C. Walker, LIDAR Thomson scattering for the ITER core plasma, in: Diagnostics for Experimental Thermonuclear Fusion Reactors, vol. 2, Plenum, New York, 1998, p. 217.
[16] T. Sugie et al., Development of multi-channel optical-fibre feed through for ITER, JAERI-Tech 98-036, August 1998.
[17] M. Finkenthal, L.K. Huang, M.J. May, H.W. Moos, S.P. Regan, A.P. Zwicker et al., Layered synthetic microstructure based diagnostics for high temperature plasma, Technical Report, Johns Hopkins University, October, 1992.
[18] S.J. Zinkle, in: Proceedings of the Seventh IEA Workshop on Radiation Effects in Ceramic Insulators, September 1993, Stresa, Italy.
[19] S.J. Zinkle, G.P. Pells, F.W. Clinard Jr., Fusion Materials Semiannual Progress Report for Period ending 30 September 1993, DOE/ER-0313/15, 1993, p. 417.
[20] F. Wedig, Berichte des Forschungszentums Julich, Jul-3334, December 1996.
[21] S.J. Zinkle et al., Fusion Materials Semiannual Progress Report for Period ending 30 June 1997, DOE/ER-0313/22, 1997, p. 179.
[22] E.R. Hodgson, J. Nucl. Mater. 179–181 (1991) 383.
[23] E.R. Hodgson, J. Nucl. Mater. 212–215 (1994) 1123.
[24] D.P. White, L.L. Snead, S.J. Zinkle, J. Appl. Phys. 834 (1998) 1924.
[25] T. Shikama, S.J. Zinkle et al., J. Nucl. Mater. 258–263 (1998) 1867.
[26] K. Noda, T. Nakazawa, Y. Oyama, D. Yamaki, Y. Ikeda, J. Nucl. Mater. 233–237 (1996) 1289.
[27] G.P. Pells, R.M. Boothby, J. Nucl. Mater. 256 (1998) 25.
[28] W. Kesternich, F. Sceuermann, S.J. Zinkle, J. Nucl. Mater. 219 (1995) 190.
[29] W. Kesternich, J. Nucl. Mater. 253 (1998) 167.
[30] O.A. Plakshin, V.A. Stepanov, P.A. Stepanov, V.M. Chernov, J. Nucl. Mater. 271&272 (1999) 496.
[31] T. Shikama, S. Yamamoto, R. Snider, M. Fukawo, T. Nishitani, K. Young, S. Kasai, M. Narui, J. Broesch, H. Matuo, T. Sagawa, Fission-reactor-radiation-tests of MI-cables and magnetic coils for fusion burning plasma diagnostics, in: Proceedings of the International Symposium of Remote Sensing, Florence, Italy, 20–24 September 1999.
[32] M. Fukawo, private communication.
[33] E. Ishitsuka, H. Sagawa, A. Nagashima et al., in: M.L. Hamilton, A.S. Kumar, S.T. Rosinski, M.L. Grossbeck (Eds.), Effects of Radiation on Materials, Proceedings of the 19th International Symposium, ASTM STP 1366, American Society for Testing and Materials, 1999, p. 1176.
[34] D.V. Orlinski, K.Yu. Vukolov, Plasma Devices and Operations 7 (1999) 195.
[35] A. Gorshkov, D. Orlinski, V. Sasnnikov et al., J. Nucl. Mater. 273 (1999) 271.
[36] A. Moroño, E.R. Hodgson, J. Nucl. Mater. 224 (1995) 216.
[37] H.N. Barr, F. Hittman, R.D. Brown, F.W. Clinard Jr., M.R.R. Lopez, H. Martinez, T.J. Romero, J.H. Cook, Fus. Technol. 17 (1990) 385.
[38] A. Nagashima, T. Fujisawa, T. Sugie, S. Kasai, Development on new vacuum windows seal for ITER optical diagnostics, in: Diagnostics for Experimental Thermonuclear Fusion Reactors, vol. 2, Plenum, New York, 1998, p. 257.
[39] A. Ibaa, R. Heidinger, J. Mollá, CVD Diamond for High Power RF, Applications in Nuclear Fusion Reactors, Electrochemical Society, Proceedings 97-32, 1998, p. 503.
[40] A.T. Ramsey, Rev. Sci. Instrum. 66 (1) (1995) 871.
[41] T. Kakuta, T. Shikama et al., Behaviour of optical fibres under heavy irradiation, in: Proceedings of the Fourth International Symposium on Fusion Nuclear Technology, MR-p36, Tokyo, 6–11 April 1997.
[42] Griscom David L, J. Appl. Phys. 80 (4) (1996) 2142.
[43] A.L. Tomashuk, K.M. Golant, E.M. Dianov et al., Radiation-induced absorption and luminescence in specially hardened large-core silica optical fibres, in: Proceedings of RADEX 99, Abbaye de Fontevraud, France, 13–17 September 1999.
[44] T. Kakuta, T. Shikama, N. Shamoto, Development of radiation-resistant optical fibres for visible application, in: Proceedings of the International Symposium of Remote Sensing, Florence, Italy, 20–24 September 1999.
[45] V.S. Voitsenya, V.I. Gritsyna, V.T. Gritsyna et al., Fus. Eng. Des. 34&35 (1997) 365.
[46] D.W. Cooke, E.H. Farnum, F.W. Clinard Jr., B.L. Bennett, A.M. Portis, Fusion Materials Semiannual Progress Report, DOE/ER, Oak Ridge National Laboratory, Oak Ridge, TN, to be published.
[47] V.M. Kosenkov et al., J. Nucl. Mater. 212–215 (1994) 1056.
[48] V.S. Voitsenya, V.G. Konovalov, M.F. Becker et al., Rev. Sci. Instrum. 70 (1999) 2016.
[49] T. Sugie, H. Ogawa, J. Katsunuma, M. Muruo, T,. Andou, S. Kasai, Design of divertor impurity monitoring system for ITER, JAERI-Tech 96-055, December 1996.